Article

Not peer-reviewed version

Anti-Hypercholesterolemia Effects of Edible Seaweeds Extracts and Metabolomic Changes in Hep-G2 and Caco-2 Cell Lines

Rita Pacheco * and Mariana Coelho

Posted Date: 9 May 2023

doi: 10.20944/preprints202305.0631.v1

Keywords: cholesterol; Eisenia bicylis; Porphyra tenera; hypercholesterolemia; metabolomics; 3-hydroxy-3-methylglutaryl coenzyme A redutase; Hep-G2; Caco-2

Article

Anti-Hypercholesterolemia Effects of Edible Seaweeds Extracts and Metabolomic Changes in Hep-G2 and Caco-2 Cell Lines

Mariana Coelho [1] and Rita Pacheco [1,2,*]

[1] Departamento de Engenharia Química, Instituto Superior de Engenharia de Lisboa (ISEL), Av. Conselheiro Emídio Navarro 1, 1959-007 Lisboa, Portugal; marycoelho98@hotmail.com

[2] Centro de Química Estrutural, Institute of Molecular Sciences, Universidade de Lisboa, 1749-016 Lisboa, Portugal

* Correspondence: ripacheco@fc.ul.pt; Tel: +351-217-500-000 (ext. 28532)

Simple Summary: Hypercholesterolemia is a major risk for the development of cardiovascular diseases, one of the main causes of mortality worldwide, and it is characterized by high plasma cholesterol levels. There are two drugs prescribed for controlling the levels of cholesterol, statins, that inhibit *de novo* biosynthesis and, ezetimibe which reduces cholesterol intestinal lining absorption. However, these drugs may have adverse effects, so new effective and safer strategies are necessary. As a still underutilized source of bioactive compounds, marine organisms are rising as possible sources of novel drugs. The aim of this work was to compare two edible seaweeds - *Eisenia bicylis* (Aramé) and *Porphyra tenera* (Nori) - regarding their anti-hypercholesterolemia effects, either as alternatives to the prescribed drugs and/or by causing positive metabolic changes. Our findings revealed that both extracts, but especially Aramé, were effective for managing hypercholesterolemia and, additionally significantly altered liver Hep-G2 and intestinal Caco-2 cell lines metabolic pathways associated to health beneficial effects. The results obtained from this work contribute to validate seaweeds intake positive impact on cardiovascular health and their use as functional foods.

Abstract: Hypercholesterolemia is a major risk for the development of cardiovascular diseases (CVDs), the main cause of mortality worldwide, and it is characterized by high levels of circulating cholesterol. The drugs currently available for hypercholesterolemia control have several side effects, so it is necessary to develop new effective and safer therapies. Seaweeds serve as sources of several bioactive compounds with claimed beneficial effects. *Eisenia bicyclis* (Aramé) and *Porphyra tenera* (Nori) are edible seaweeds which were previously recognized as rich in bioactive compounds. In the present study, we aim to evaluate the anti-hypercholesterolemia effect of these two seaweeds extracts and their health potential. Both extracts, but more efficiently Aramé extract demonstrated to have liver 3-hydroxy-3-methylglutaryl coenzyme A reductase (HMGR) inhibitory activity and to reduce approximately 30 % cholesterol permeation through human Caco-2 cells simulating the intestinal lining, targets for hypercholesterolemia treatments. An untargeted metabolomic assay on human intestinal Caco-2 and liver Hep-G2 cells lines exposed to Aramé and Nori extracts revealed changes in the cell's metabolism as indicators of the extract's health beneficial effects. The metabolic pathways affected by exposure to both extracts were associated to lipid metabolism, such as phospholipids, and fatty acid metabolism, pathways of amino acid, cofactors and vitamins and cellular respiration metabolism. More profound for Aramé treated cells, but also seen for Nori exposed cells, the metabolites modifications were associated with the protection against CVDs and other diseases and, to the improvement of cells oxidative stress tolerance. The results obtained for the anti-hypercholesterolemia properties, in addition to the revelation of the positive impact on cells metabolism, are an important contribution for further evaluation of these seaweeds extracts as functional foods or for CVDs prevention.

Keywords: cholesterol; *Eisenia bicylis*; *Porphyra tenera*; hypercholesterolemia; metabolomics; 3-hydroxy-3-methylglutaryl coenzyme A reductase; Caco-2; Hep-G2

1. Introduction

According to the World Health Organization (WHO), cardiovascular diseases (CVDs) are the leading cause of mortality, both in industrialized and developing countries [1]. In 2019, around 17.9 million people died from CVDs, representing 32 % of the world global deaths. By 2030 it is estimated that at least 24 million people may die, mainly from heart attack and stroke [1,2].

Hypercholesterolemia is a key factor for the development of CVDs and, therefore the major target of risk reduction programs [3,4]. It's characterized by high level of low-density lipoprotein cholesterol (LDL) and very low-density lipoprotein (VLDL), or triglycerides, and the decrease of high-density lipoprotein (HDL) [5,6]. Tough, cholesterol is a lipid that plays a crucial role in many biochemical and biophysical processes, having an irreplaceable role in human health, high levels of circulating cholesterol in the blood is a disorder of metabolism and/or nutrition [7]. These high levels of cholesterol may promote atheromatous plaques deposits in arteries, a condition known as atherosclerosis, leading to a series of complications, from inflammation, high blood pressure, coronary heart disease and other disorders to fatal thromboembolic events [8].

Cholesterol homeostasis in the organism is mainly maintained by three routes, endogenous cholesterol synthesis, diet or exogenous cholesterol intestinal absorption and excretion, and cholesterol hepatic excretion [9]. Cholesterol *de novo* biosynthesis occurs both in the intestine and in the liver, by a pathway where the major regulatory enzyme is 3-hydroxy-3-methyglutaryl coenzyme A reductase (HMGR). Cholesterol exogenous absorption occurs via Niemann-Pick C1 Like 1 (NPC1L1) protein and other ABC transporters located in the apical membrane of enterocytes [5,10]. Human liver also expresses NPC1L1 and ABC transporters, these are in the canalicular membrane facilitating cholesterol uptake in hepatic cells for biliary cholesterol excretion (reverse cholesterol transport) [5,10].

NPC1L1 protein is the molecular target of ezetimibe, often prescribed for reducing the small intestine cholesterol uptake [11]. Though life-threatening liver failure is rare with this drug [12] ezetimibe, used in monotherapy, has low efficacy reducing the circulating cholesterol by only 15-20% [13,14]. Therefore, ezetimibe is often prescribed in combination with statins for controlling hypercholesterolemia [7]. Statins are a family of compounds prescribed as HMGR enzyme inhibitors [12], with different behavior regarding its absorption, bioavailability, excretion, binding to plasmatic proteins and lipophilicity, however most having considerable side effects [15]. Statins are well tolerated but may promote hepatotoxicity or kidney toxicity and other adverse effects such as diabetes mellitus type 2, specific effects on muscles, neurologic and neurocognitive effects [16,17].

Even though the mechanisms of resistance and adverse effects to hypercholesterolemia treatment are not fully elucidated, the medical and scientific community points out the urgent need to identify individuals who are more likely to experience drug side effects and/or to find alternative therapies to the available drugs [15,18,19].

The combination of natural products intake with anti-hyperlipidemic drugs is a rising strategy [20,21], mostly because numerous cases of cholesterol imbalance are a consequence of bad dietary habits and, it is widely accepted that a healthy diet contributes to cardiovascular health [2]. Natural products are known to be rich in bioactive compounds [22] so there has been a growing interest in their use for improving health and wellness to reduce metabolic risk factors, in particular hypercholesterolemia [23].

As a still underutilized source of interesting bioactive compounds, marine organisms are rising as possible suppliers of novel drugs [24]. In the literature, algae have been mentioned as having great potential bioactive against several human health concerns [25] so having prospective application as functional food ingredients, nutraceutical or drugs, thus high economic importance.

 doi:10.20944/preprints202305.0631.v1

Nevertheless, seaweeds, also known as macroalgae [26], have a long history in the Southeast Asian Regions, such as China, Japan and South Korea were they are traditionally consumed [27]. Evidence from epidemiological research suggests that regular seaweed consumption lowers the incidence of chronic diseases, such as cancer, cardiovascular diseases, and related risk factors in these parts of the world [28].

Owing to a healthier diet profile, seaweeds consumption is increasing in Western and European countries where they are considered as novel functional foods, with claims of prolonging lifespan and prevention of CVDs [29]. Seaweeds are also an abundant and sustainable marine resource and an alternative to animal products as they are a rich source of macro and micronutrients [30]. The micronutrients are minerals, namely iron and magnesium and lipid or water-soluble vitamins. Regarding macronutrients, seaweeds are rich in proteins and sulphate-polysaccharides [31]. These nutrients are essential for human nutrition and development and additionally some may have health impacts [32].

Seaweeds are taxonomically classified into three main groups, brown seaweeds (phylum *Ochrophyta*), red seaweeds (phylum *Rhodophyta*) and green seaweeds (phylum *Chlorophyta*) [29]. The colors of the seaweeds are associated with the pigments such as chlorophyll for green, phycobilin for red, and fucoxanthin for brown seaweeds [33]. *Eisenia bicyclis*, traditionally known as Aramé [34], is a perennial brown seaweed, which belongs to the phylum *Ochrophyta*, class *Phaephyceae*, order *Laminariales* [29], family *Laminariaceae* and is distributed along the mid-Pacific coastlines of Korea and Japan [34]. Arame seaweed is popular in Asian cuisine for soups and salads [35,36]. *Porphyra tenera,* traditionally known as Nori, is a red seaweed that belongs to the phylum *Rhodophyta*, class *Rhodophyceae*, order *Bangiales* and family *Bangiaceae* [37] and is considered as one of the most popular edible seaweeds, since it's use in sushi and soups [38].

In this work, extracts from these seaweeds were evaluated for their potential against hypercholesterolemia, namely the capacity to inhibit HMG-CoA reductase and the cholesterol permeation in an in vitro model of the intestinal lining using Caco-2 cells. Considering that these seaweeds are often incorporated in the diet and, in order to better understand their health potential, this study was complemented with an analysis of the extract's effects *in vitro*, on liver Hep-G2 and intestinal Caco-2 cell lines. In particular, liver and intestinal cell lines metabolites were seen to be affected due cells exposure to the complex mixture of bioactive compounds in the extracts. Understanding the activity of these seaweeds' extracts over biological systems, in these case cell lines, is very important in order to explain the induced effects, revealing its bioactives' mechanisms of action and how these modulated metabolic pathways, mainly those associated to hypercholesterolemia and CVDs.

To the best of our knowledge, no study or literature evaluated in more detail, at the same time, the *Eisenia bicyclis* extract (Aramé) and *Porphyra tenera* extract (Nori), regarding their effect on hypercholesterolemia and its effect in intracellular metabolites to explain its mechanism of action.

2. Materials and Methods

Both the dried *Porphyra tenera* (Nori) seaweed biomass, from the Blue Dragon line of the Flavers-International Flavours Shop (B#JS2039J01), and *Eisenia bicyclis* (Arame) seaweed biomass, from the Seara brand (B# T20220405), were purchased in a local store.

2.1. Chemicals

All solvents were of analytical grade unless otherwise specified and used without further purification. Roswell Park Memorial Institute (RPMI-1640), Dulbecco's Modified Eagle Medium (DMEM), trypsin and glutamine from Biowhittaker® Lonza. Fetal Bovine Serum (FBS) from Biowest, phosphate-buffered saline (PBS) from Corning (Corning, NY, USA). Antibiotic Antimycotic Solution 100x (10 000 U/mL penicillin, 10 mg/mL streptomycin and 25 µg amphotericin B/mL), cholesterol and HMGR assay kit from Sigma®Aldrich (St. Louis, MO, USA).

Preprints (www.preprints.org) | NOT PEER-REVIEWED | Posted: 9 May 2023 doi:10.20944/preprints202305.0631.v1

2.2. Preparation of Arame and Nori Seaweeds Extract

The procedure for obtaining a dried mass of Nori extract (50 % g/g yield), by a decoction in water of 20 g *Porphyra tenera* biomass /L, was similar to a procedure already reported by our group [19] for obtaining the dried mass of Aramé extract by a decoction of 33 g *Eisenia bicyclis* biomass /L of water (66% g/g yield). In a recent report form the authors [25], the aqueous extracts from these seaweeds were characterized according to its composition in total phenolic, proteins and polysaccharides content and, the mixture of compounds present was identified by liquid chromatography coupled to high resolution mass spectrometry The identification of the bioactive compounds in these extracts showed that these contained different mixtures of phlorotannins, i.e phloroglucinol polymers [25]. Aramé extract was seen to have a higher content in total phenols and to be mixture of eckol and fucol derivatives type of phlorotannins' derivatives. As for Nori extract it was seen to contain a higher amount of fucol type phlorotannins.

2.3. Cell Lines Cultures

Hepatocellular carcinoma cell line (Hep-G2) and colorectal adenocarcinoma cell line (Caco-2) were cultured in DMEM and RPMI-1640 medium, respectively, supplemented with 10 % (DMEM) and 20 % (RPMI-1640) of inactivated FBS, 5 mL of antimycotic and 5 mL of L-glutamine at 37 ^{0}C in an atmosphere with 5 % CO_2. The medium was changed every 48-72 hours, and cells were trypsinized before reaching confluence using trypsin 1x.

2.4. Inhibition of Enzyme HMG-CoA Reductase (HMGR)

To determine HMGR inhibition, the procedure described in the assay kit was followed. In this assay, the decrease in NADPH (Nicotinamide Adenine Dinucleotide Phosphate reduced) absorbance was measured in the presence of HMG-CoA substrate. The initial rate of the enzymatic reaction was quantified by measuring the absorbance at 340 nm for 3 min (V[compound]). A control reaction was carried out using water, instead of the extract solution and this initial rate which was considered 100 % of the enzymatic activity, Vcontrol. The percentage of HMGR inhibition (I) for the extracts was determined as the ratio of V[compound] and Vcontrol. All the assays were carried out in triplicate. The concentration of the extracts used in the reaction mixture was 0.25 mg/mL.

2.5. In Vitro Studies in Caco-2 Cells Monolayers Simulating the Intestinal Lining

For these assays, Caco-2 cells were seeded in 12-well transwell microplate inserts (BD FalconTM) at a density of $5x10^4$ cells/cm^2, as described in [39]. The monolayers were formed and differentiated by approximately 23 days. The medium was replaced every 48 hours. The monolayer formation was confirmed when reaching a trans-epithelial electrical resistance higher than 250 Ω/cm^2, measured using a Millicell ERS-2 V Ohm (Millipore).

2.5.1. Cholesterol Permeation Assay

To start the assay the Caco-2 cell monolayers were washed with Hank's Balanced Salt Solution (HBSS). Afterwards the cells monolayers were incubated for 6 h with 5 mM cholesterol and adding either 100 mM ezetimibe, 0.3 mg dried mass extract /mL HBSS or both. These assays were performed three times and compared with control cells only incubated with HBSS solution.

After 6 hours of incubation, the solutions from both the apical side and basolateral chamber were collected and 75 µL aliquots were analyzed by RP-HPLC-DAD (VWR HITACHI, with a detector L-2455, oven da column L-2300, autosampler L-2200 e a pump L-2130). The separation was carried out in an isocratic mode using 50 % methanol plus acetonitrile for 15 minutes with a flow of 1 mL/minute. The percentage of cholesterol permeation was determined assuming that 100 % cholesterol permeation occurred when cells were incubated for 6h only in the cholesterol presence.

 doi:10.20944/preprints202305.0631.v1

2.5.2. Seaweeds Compounds Permeation Assay

Caco-2 cells monolayers were incubated for 6 h with 0.3 mg dried mass extract /mL HBSS and after the solutions from both the apical side and basolateral chamber were collected and 25 µL further analyzed by RP-HPLC-DAD. The separation was carried using a gradient of trifluoroacetic acid (TFA) (0.05 %) and acetonitrile (ACN) for 55 minutes with a flow of 0.8 mL/minute as follows: 0 min, 100% TFA; 30 min, 70% ACN, 30% TFA; 40 min, 20% TFA, 80% ACN; 50 min 70% ACN, 30% TFA; A; 55 min 100% TFA. The percentage of seaweed compounds permeation was calculated by the height of the most intense seaweed peak, assuming that 100% corresponds to the 0.3 mg/mL extract solution in HBSS. These assays for performed three times and compared with control cells incubated only with HBSS solution.

2.7. Metabolomic Analysis of Caco-2 and Hep-G2 Cells Treated with Seaweeds Extract

Hep-G2 cells were grown in T25 flasks, as previously described, to reach confluence. Caco-2 cells were also cultivated in T25 flasks, as described previously, allowed to reach confluence and afterwards differentiated.

Both cells were incubated with 0.3 mg seaweed extract dried mass/mL of growth medium for 24 h at 37 ^{0}C in an atmosphere with 5 % CO_2. Control assays only cells incubated only in growth medium were additionally performed. After 24 h, the cells were washed with PBS and cells collected for metabolites extraction using an adaptation of a procedure described in [40].

The extracted metabolites were analyzed using liquid chromatography (LC) in an UHPLC ELUTE autosampler coupled to high resolution mass spectrometry (HRMS) in Impact II QToF (Quadruple Time of Flight) mass spectrometer equipped with an electrospray source (ESI) from Bruker (Bruker DaltoniK GmbH, Bremen, Germany). Extracted metabolites were injected (5 µL) in an UHPLC chromatographic column Intensity Solo 2 RP-18, 100 × 2.1 mm, 2.0 µm column (Bruker, Bremen, Germany). The column was kept at 35°C and the samples at 10°C. A gradient of water with 0.1% formic acid (eluent A) and acetonitrile with 0.1% formic acid (eluent B) was used at a flow rate of 0.250 mL/min as follows: 0 min – 95% A; 1.5 min – 95% A; 13.5 min – 25% A; 18.5 min – 0% A; 21.5 min – 0% A; 23.5 min – 95% A; 30 min – 95% A. High resolution mass spectra were acquired in ESI positive and negative modes. Mass spectra were acquired, in the range of 120-1000 m/z and the mass spectrometer parameters were adjusted to optimize the signal-to-noise (S/N) ratio for the ions of interest. Briefly, −3.5 kV and +4.0 kV; end plate offset, 500 V, nebulizer gas (N_2) 2.0 bars; dry gas (N_2), 8 Lmin-1; dry heater, 200 °C; collision cell energy was set to 5.0 eV. The internal calibration was performed with 250 mL H_2O, 50 mL iPrOH, 750 µL acetic acid, 250 µL formic acid, and 0.5 mL 1N NaOH solution on HPC mode. The acquired data were processed and compared by MetaboScape® 4.0 software (Bruker Daltonik GmbH, Bremen, Germany). For replicates were made for each condition.

Metabolites for cells incubated with the extracts were listed by their charge/mass (m/z) ratio, retention time and abundance, either in terms of signal intensity or area. The metabolites (retention time-m/z pairs) from cells exposed to each seaweeds extract were statistically compared with listed metabolites (retention time-m/z pairs) from control cells. MetaboScape program generates of a statistical analysis and the metabolites considered as having a significant variation between the control and the cells treated with the extract were those presenting the significance level at *p-value* < 0.05 and fold change below 0.5 and above 1.7.

Multivariate statistics of metabolites, such as principal component analysis (PCA) [41] was performed to evaluate the degree of metabolic differences between groups, i.e., control cells versus cells exposed to the extract, but also the similarity between the assayed replicates (n=4). Other statistical analysis was applied to assess whether the detected differences in the metabolites were statistically significant between the compared groups. Volcano plots were represented as the $\log_2$ mean fold changes in the abundance of the metabolites between the control cells and the extract exposed cells plotted against -$\log_{10}$ (p-value). The metabolites showing a *p-value* lower than 0.05 and a fold change between 0.5 and 1.7 were considered significant. Projection on Latent Structures (PLS) regression were additionally applied using MetaboScape to identify similarities and differences in

Preprints (www.preprints.org) | NOT PEER-REVIEWED | Posted: 9 May 2023 doi:10.20944/preprints202305.0631.v1

metabolites and/or intensities of the cellular metabolites in control cells relative to the extract exposed cells assigning the importance of the altered metabolites depending on the variation found. The variable importance is a measure of the contribution of each individual metabolite for the separation between groups [41]. The cell metabolites from both groups were tentatively identified using the databases such as PubChem, HMDB and Metlin. Additionally, an analysis of the metabolic pathways associated with the changes identified in the metabolites was performed using as tool MetaboAnalyst 5.0.

2.9. Data Analysis

The software used for treatment was Microsoft® Excel (Microsoft Office 365) and the results were expressed as average ± standard deviation. Additional analysis of variance was done using a one-way ANOVA for values comparison, difference between mean values were considered significant when $p < 0.05$.

3. Results

3.1. Seaweeds Extracts Anti-Hypercholesterolemia Effects

3.1.1. Inhibitory Effect on HMG-CoA Reductase (HMGR)

As previously mentioned, the enzyme HMGR is the key enzyme of the cholesterol *de novo* biosynthesis and a target for treatment of hypercholesterolemia [11]. Synthetic drugs, statins, are commonly prescribed, but due to its side effects novel drugs are needed. In addition to lovastatin, which is the first drug to hit the market, there are six other statins available to date: simvastatin, pravastatin, fluvastatin, atorvastatin, rosuvastatin and pitavastatin [42].

The potential of marine origin products for the treatment of hypercholesterolemia is still largely unexplored, though there are several that showed or are claimed for having lipid lowering activities [43]. In order to clarify *Porphyra tenera* (Nori) and *Eisenia bicyclis* (Aramé) extracts under study, may affect cholesterol *de novo* biosynthesis, HMGR inhibitory activity of these extracts was evaluated and compared with pravastatin. Though there were previously reported results by our group for Aramé extract [19] to the best of our knowledge this is the first report for Nori extract. The results for 0.25 mg/mL solution of Nori dried extract, Aramé extract at the same concentration [19] and pravastatin drug are showed in Table 1. The Nori extract exhibits lower inhibition capacity than the Aramé extract with 79 % HMGR inhibition and, furthermore the positive control, pravastatin, 95 % enzyme inhibition. The high value of HMGR inhibition of Aramé extract, as a natural product extract, may reflect the strong potential of edible Aramé seaweed for the reduction of cholesterol levels, as a functional food targeting hypercholesterolemia.

Regarding the differences in the bioactive compounds present in these extracts, the Aramé extract has, as previously seen, higher content in phenolic compounds and eckol type phlorotannin's, than Nori extract [25]. Previous work with brown seaweeds such as *Ecklonia stolonifera* also reported the effect in rats of this eckol and dieckol containing extracts as anti-hyperlipidemic agents [44].

Table 1. HMG-CoA reductase (HMGR) inhibitory activity of 0.25 mg/mL *Eisenia bicyclis* extract (Aramé), 0.25 mg/mL *Porphyra tenera* extract (Nori) and pravastatin.

	HMGR inhibitory activity (%)
Nori	41 ± 3^{a}
pravastatin	95 ± 1^{b}
Aramé [19]	79 ± 7^{c}

Superscript letters (a-c) correspond to values that are statistically different between the samples under study ($p < 0.05$).

Preprints (www.preprints.org) | NOT PEER-REVIEWED | Posted: 9 May 2023 doi:10.20944/preprints202305.0631.v1

3.1.2. Effects on Cholesterol Permeation In Vitro through Human Caco-2 Cells

Human epithelial colorectal adenocarcinoma cells, Caco-2, are well characterized intestinal in vitro model with morphologic resemblance to intestinal epithelia [45]. When cultured under appropriate conditions this cell model is accepted as a surrogate for human intestinal permeability measurements by the regulatory agencies like FDA and EMA, and also as a screening tool for intestinal absorption, transport, and metabolism in support of drug discovery [46].

In order to compare the impact of the two seaweed extracts in the intestinal cholesterol absorption, Caco-2 cells were cultured as a monolayer and allowed to differentiate for 21 days, simulating the human intestinal epithelial membrane. The differentiated cells permeability to cholesterol was assessed in the presence of the extracts and both in the absence or presence of ezetimibe (Ezet.), the drug prescribed for reducing diet cholesterol permeation. Ezetimibe was used also alone as a positive control. Figure 1 shows the results, after 6 h incubation with cholesterol, of the percentage of reduction in cholesterol permeation at the different conditions tested. The permeability of cholesterol alone through the differentiated cells was considered 100 % permeation.

It can be seen in Figure 1, that the drug ezetimibe (Ezet.) reduced 52 % cholesterol permeation through the Caco-2 cells and, a similar effect, was obtained when cells were in contact with ezetimibe besides Aramé extract (Aramé+Ezet.). The incubation of the cells solely with any of the extracts, Aramé or Nori, only reduced cholesterol permeation by approximately 30 %. Though these values are below the effect of drug ezetimibe, these results are considered promising as the extracts are a mixture of several compounds. Therefore, the compounds on the extracts have a promising potential for lowering cholesterol permeation in the intestinal lining, contributing for control of dietary cholesterol absorption.

This is the first report demonstrating Nori extract ability to inhibit cholesterol permeation in Caco-2 cells, a model of the intestinal lining. However, it can be seen in Figure 1, that in the presence of ezetimibe plus Nori (Nori+Ezet.), a lower percentage of reduction in cholesterol permeation was reached (24 %) than using ezetimibe alone (52%), anticipating Nori extract interfering with ezetimibe drug effect. The awareness of interactions of seaweed compounds with drugs is limited to a few studies, mostly with anticancer drugs [47,48], however this is an important issue that needs to be carefully addressed considering edible seaweeds such as Nori are often used in the diet.

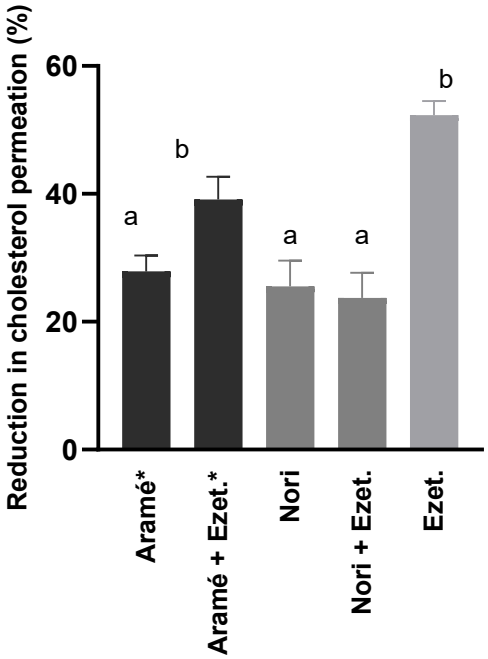

Figure 1. Reduction of cholesterol permeation, through Caco-2 cells monolayer, with extracts of Aramé and Nori. Ezetimibe (Ezet.) was used as a positive control. Caco-2 cells were differentiated for

Preprints (www.preprints.org) | NOT PEER-REVIEWED | Posted: 9 May 2023 doi:10.20944/preprints202305.0631.v1

21 days and incubated with 5 mM cholesterol during 6 h. Cholesterol was quantified using RP-HPLC-DAD as mentioned in section 2.5. a-b corresponds to values that are statistically different between de samples under study ($p < 0.05$). * results in [19].

3.1.3. Seaweed Extracts Permeation In Vitro through Human Caco-2 Cells

A permeability assay was also conducted to evaluate whether the extracts compounds permeated the gastrointestinal barrier. The results are shown in Figure 2. Overall, the results revealed that the major compounds of the analyzed seaweed extracts permeated Caco-2 cells, simulating the human intestinal epithelial membrane, by less than 30 %. Considering the nature of the bioactive compounds composing the extracts, mostly lower molecular weight phlorotannin's derivatives [25] it was expected that these permeate the intestinal barrier [49,50].

These findings are significant, so suggesting that in vivo the extract compounds have the potential for permeating the gastrointestinal barrier, and moving towards other body cells, tissues, or organs, ultimately successfully reaching the liver where HMGR may be inhibited, as described in Section 3.1.1. Due to the ability of the extract compounds to permeate barriers, it seemed appropriate to further explore the impact of these seaweeds extracts in the metabolism, using both Caco-2 cells and human liver hepatoblastoma-derived cell line Hep-G2 cells.

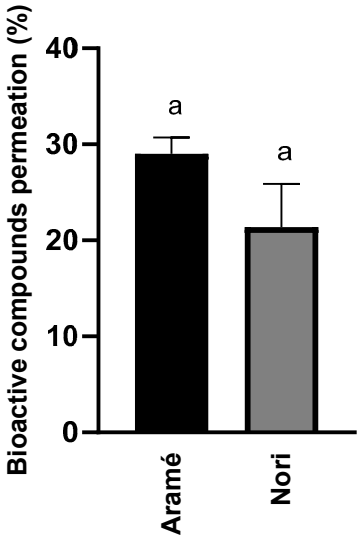

Figure 2. Permeation of bioactive compounds through Caco-2 cells monolayer of Aramé and Nori extracts in presence of cholesterol. Caco-2 cells were differentiated for 21 days and incubated with the extract during 6 h, after 6 h extracts were quantified using RP-HPLC-DAD as mentioned in section 2.5. Letters a, correspond to values that are not statistically different between the samples under study ($p < 0.05$).

3.2.3. Metabolomic Effect of Seaweed Extract on Caco-2 and Hep-G2

To evaluate the mode of action and potential health effects of edible seaweeds extracts intake, an untargeted liquid chromatography associated with high-resolution mass spectrometry (LC-QTOF-MS) metabolomics analysis was performed. The aim of this approach was to identify key metabolites and metabolic pathways modified in liver Hep-G2 cells and intestine Caco-2 cells in response to exposure to the extracts.

- Aramé extract

Caco-2 cells metabolites (Control) were compared with the metabolites from Caco-2 cells incubated in the presence of the Arame extract. After the statistical analysis of the list of metabolites collected by mass spectrometry, either in the MS positive or negative mode, (Supplementary Information, Figure S1) the statistically different putative metabolites were recognized and several

Preprints (www.preprints.org) | NOT PEER-REVIEWED | Posted: 9 May 2023 doi:10.20944/preprints202305.0631.v1

were tentatively identified using databases such as PubChem, HMDB and Metlin. In the heatmaps, showed in Figures 3A and 4A for the MS positive and negative mode respectively, the most abundant identified metabolites are represented in green towards the less abundant metabolites are shown in red. Figures 3B and 4B show for the putative identified metabolites the relative abundance (log_2 (fold change)) between control cells (blue) and the Caco-2 cells in contact with Aramé extract (orange).

Caco-2 metabolites MS positive mode	Control	Aramé
O4-[4-[(E)-2-(3-hydroxy-5-methyl-phenyl)vinyl]phenyl] ester O1-(2-keto-3,5,5-trimethyl-4-vinyl-cyclohex-3 -en-1-yl) ester Succinic acid (O4)	3254	98
Glutathione (GSH)	97111	3612
(1,4-dimethyl-4-propylheptyl)-(2-methylbutyl)amine (DPHMA)	464590	31263
Phosphatidylethanolamine (PE 16)	12449	3408
Adenylosuccinate (ADS)	25171	3170
1-[2-[[1-[2-[[2-[[2(glycylamino)acetyl]amino]acetyl]amino]acetyl]amino]acetyl]prolyl]amino]-5-guanidino-pentanoyl]proline (AGP)	45337	7552
1-Palmitoylphosphatidylcholine (PPC)	25622	6572
1-Monopalmitin (MPN)	125685	25283
Benzylpenicilloyl-Cysteine (BPO-Cys)	84964	6740
Cyclohexanecarboxylic acid [2-hydroxy-3-(isopropylamino)propyl] ester (CHC)	13774	425
1-(9Z-Octadecenoyl)-sn-glycero-3-Phosphoethanolamine (PE 18)	14283	5468
3-amino-2,3-dideoxy-scyllo-inosose (ADSI)	1426	67543
Hypoxanthine (HPX)	48934	331014
(1S,2R)-1-[3-(methylthio)-1H-pyrazol-5-yl]propane-1,2,3-triol (Triol)	1362	58389

Caco-2 metabolites MS positive mode	Control	Aramé
Inosine (I)	32804	221444
Spermin (Spe)	538	32471
1-[5-(Benzylthio)-1,3,4-thiadiazol-2-yl]-5-(3,4-diethoxyphenyl)-4-[2,3-dihydro-1,4-benzodioxin-6-yl (hydroxy)methylene]pyrrolidine-2,3-quinone (Quin)	574	18014
ʾbamic (2-keto-2-thiazolidin-3-yl-ethyl) acid (Carbamic)	2681	44430
(2S)-1 - [(2S)-2-(mercaptomethylamino)propanoyl]proline (Proline)	1189	16298
(2R,4S)-2-[(1R)-2-[[2-[(2-amino-2-carboxy-ethyl)disulfanyl]-1-carboxy-ethyl]amino]-2-keto-1-[(2-phenylacetyl)amino]ethyl]-5,5-dimethyl-thiazolidine-4-carboxylic acid (Carb)	3515	28431
Succinyl Adenosine (SAD)	23012	109916
Cys-Pro	1408	39137
N-Propionylmethionine (N-P)	5073	14371
L-Norleucine (L-N)	119588	339655
3-[7-[4-(2-acetamido-4-methyl-thiazol-5-yl)sulfonylpiperazino]-5-methyl-[1,2,4]triazolo[1,5-a]pyrimidin-6-yl]ethyl ester propionic acid (Prop)	2997	194426
Choline (CHO)	154823	320119

(**A**)

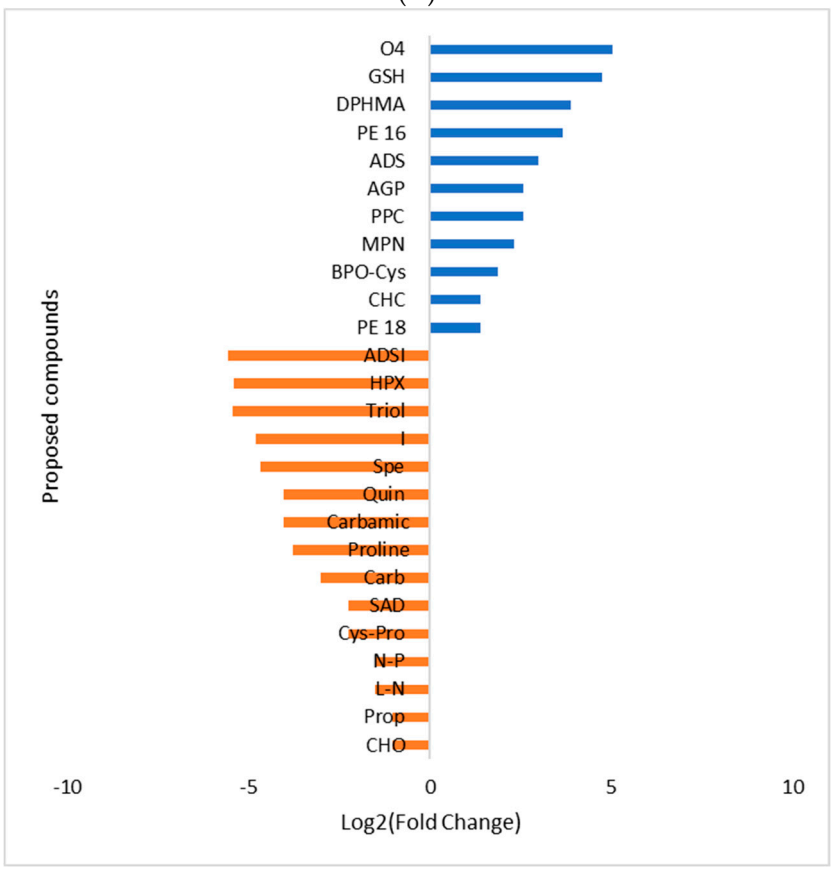

(**B**)

Figure 3. (A) Heatmap of intensity of the identified metabolites in positive mode that vary in the presence or absence of Aramé, in Caco-2 cells, based on mean intensities ($p < 0.05$). Control is Caco-2 cells only with culture medium and Aramé is the Caco-2 cells in contact 24 h with 0.3 mg/mL of Aramé extract. (B) Log_2(Fold Change) represents the ratio in the intensity of the metabolites that are increase in control relatively to Aramé treated cells, positive values in blue, negative in orange.

Preprints (www.preprints.org) | NOT PEER-REVIEWED | Posted: 9 May 2023 doi:10.20944/preprints202305.0631.v1

Caco-2 metabolites MS negative mode	Control	Aramé
PG(22:6(4Z,7Z,10Z,13Z,16Z,19Z)/0:0) (PG22)	19265,5	767
1-(2-Methoxy-octadecanyl)-sn-glycero-3-phosphoserine (MPS)	23058	1049,5
2-arachidonyl-sn-glycero-3-phosphoethanolamine (AGPE)	6986,5	482,5
PE(18:1(9Z)/0:0) (PE18)	13092,5	1388
lysophosphatidylethanolamine (LPE)	12199,5	1584,5
5-hydroxyeicosatetraenoic acid (5-H)	145634	19471,5
1-[1-(2-Dodekoxyethoxy)ethoxy]ethyl hydrogen sulfate (DHES)	48977	6739,5
2-[3-[3-[3-(3-Octoxypropoxy)propoxy]propoxy]propoxy]ethyl hydrogen sulfate (OPHES)	27328	4075
C75 trans (C75)	43338	7634
1-nonadecanoyl-glycero-3-phosphoserine (NGPS)	66979	9367
2E-Hexenedioylcarnitine (2H-E)	17532,5	3283
1-hexadecyl-sn-glycero-3-phosphoethanolamine (HGPE)	8704,5	1644
2-keto-N-[6-(4-neopentylpiperazino)-3-pyridyl]-2-(2-phenyl-5,6,7,8-tetrahydroindolizin-3-yl)acetamide (Acetamide)	73430	18972
4-Nitrophenol (4-NF)	2854	765

Caco-2 metabolites MS negative mode	Control	Aramé
16-Hydroxy-hexadecanoic acid (16 -HH)	3502	1078
Cetoleucine (Cet)	58869	18238
1,11-Undecanedicarboxylic acid (UCA)	6682	2245
Adenosine diphosphate (ADP)	93313	31714
Undecanedioic Acid (UA)	5123	2111
3-hydroxy-3-methyl-glutaric acid (HGA)	16937	7723
1-(3-Ethylsulfinylcyclohexyl)-2-methyl-3-[2-[(5-methyl-2-thienyl)sulfonylamino]ethyl]guanidine (G)	9234	4249
guanosine monophosphate (AMP)	18542	9722
Guanosine (GN)	36560	19089
2-[1-(Methyldisulfanyl)ethyl]pyrazine (MEP)	312	8962
Deoxynosine (D)	832	4440
2-[[2-acetamido-3-carboxy-propanoyl]amino] succinic acid (SA)	2366	12493
Uridine (U)	7107	35622
H-Ala-Ala-Thr-Lys-Ala-Thr-Ala-al (A-A-T-L-A-T-A)	1085	3395
H-Gly-Ser-Ala-Lys-Tyr-Gln-OH (G-S-A-L-T-G)	1407	3815

(**A**)

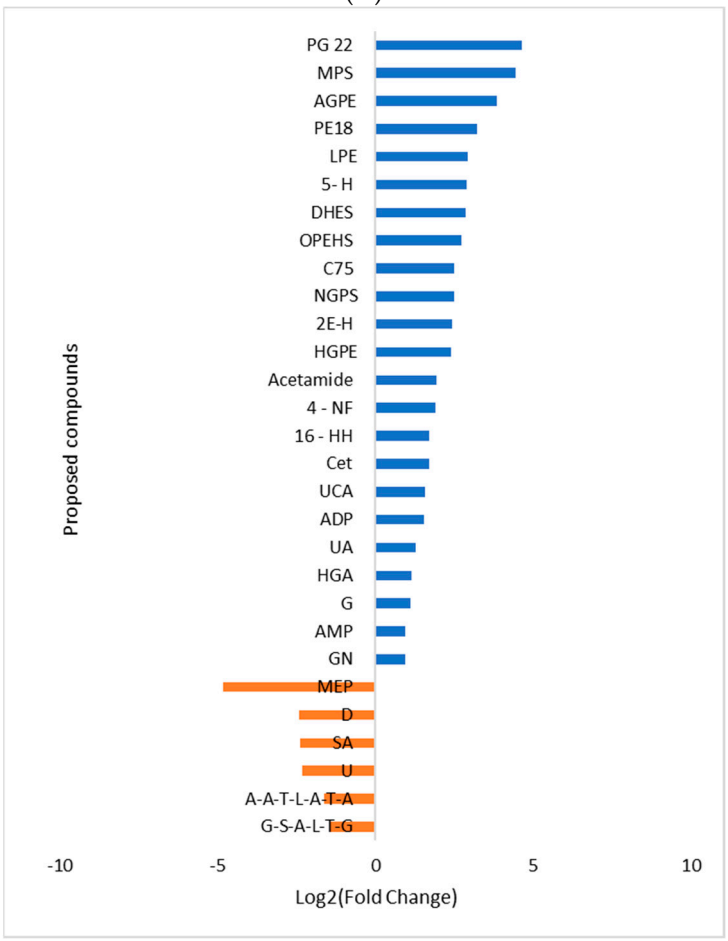

(**B**)

Figure 4. (A) Heatmap of intensity of the identified metabolites in negative mode that vary in the presence or absence of Aramé, in Caco-2 cells, based on mean intensities ($p < 0.05$). Control is Caco-2 cells only with culture medium and Aramé is the Caco-2 cells in contact 24 h with 0.3 mg/mL of Aramé extract. (B) Log_2(Fold Change) represents the ratio in the intensity of the metabolites that are increase in control relatively to Aramé treated cells, positive values in blue, negative in orange.

The same type of analysis and data treatment was made for liver Hep-G2 cells exposed to the Aramé extract. The cell modified metabolites were extracted, MS analyzed in both positive and negative mode and compared with the metabolites from non-exposed control cells. After the

Preprints (www.preprints.org) | NOT PEER-REVIEWED | Posted: 9 May 2023 doi:10.20944/preprints202305.0631.v1

statistical analysis (Supplementary Information, Figure S2), the heatmaps of the statistically significant differently abundant metabolites between control cells and Aramé exposed cells were tentatively identified and the differences can be seen in Figures 5A and 6A for MS positive and negative mode, respectively. Figures 5B and 6B show for the putative identified metabolites the difference in relative abundance (log2 (fold change)) between Hep-G2 control cells (blue) and Hep-G2 cells in contact with Aramé extract (orange).

Hep-G2 metabolites MS positive mode	Control	Aramé
L-phenylalanyl-L-threonyl-L-glutaminyl-L-seryl-L-leucyl-L-prolyl-L-proline (Phe-Pro)	9805	171
6-O-sinapoyl-D-glucone-1,5-lactone (Lactone)	10046	253
Thiamine (B1)	9766	2106
Glutathione (GSH)	94977	23142
(1,4-dimethyl-4-propylheptyl)-(2-methylbutyl)amine (DPHMA)	107692	33266
5'-methylthioadenosine (5'-Deoxy-5')	52084	18237
(2R,4S)-2-[(1R)-2-[[2-[(2-amino-2-carboxy-ethyl)disulfanyl]-1-carboxy-ethyl]amino]-2-keto-1-[(2-phenylacetyl)amino]ethyl]-5,5-dimethyl-thiazolidine-4-carboxylic acid (Carb)	3635	13179
1-[5-(Benzylthio)-1,3,4-thiadiazol-2-yl]-5-(3,4-diethoxyphenyl)-4-[2,3-dihydro-1,4-benzodioxin-6-yl (hydroxy)methylene]pyrrolidine-2,3-quinone (Quin)	1043	3367
3-amino-2,3-dideoxy-scyllo-inososе (ADSI)	3756	9035
Spermin (Spe)	2339	5279
ε-Caprolactam (ε-C)	403457	905487
3-[7-[4-(2-acetamido-4-methyl-thiazol-5-yl)sulfonylpiperazino]-5-methyl-[1,2,4]triazolo[1,5-a]pyrimidin-6-yl]ethyl ester propionic acid (Prop)	66625	148527
Cys-Pro	5893	10909
(2S)-1 - [(2S)-2-(mercaptomethylamino)propanoyl]proline (Proline)	3715	6265

(**A**)

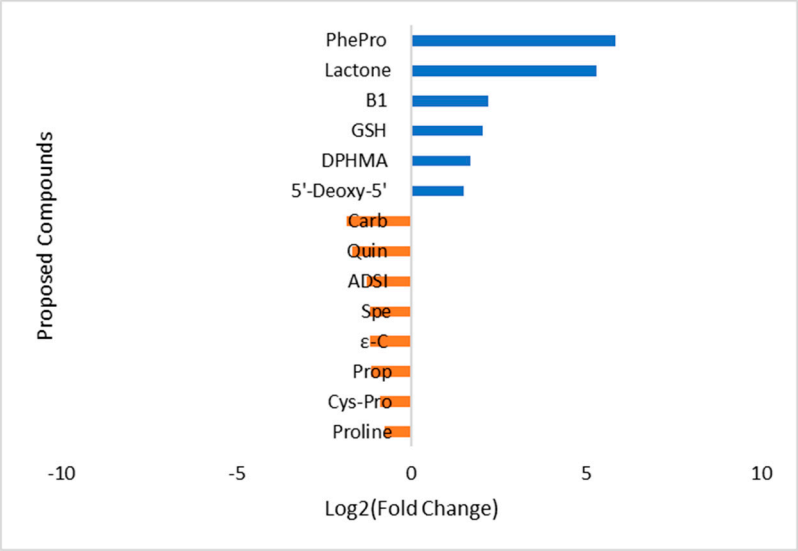

(**B**)

Figure 5. (A) Heatmap of intensity of the identified metabolites in positive mode that vary in the presence or absence of Aramé, in Hep-G2 cells, based on mean intensities ($p < 0.05$). Control is Hep-G2 cells only with culture medium and Aramé is the Hep-G2 cells in contact 24 h with 0.3 mg/mL of Aramé extract. (B) Log_2(Fold Change) represents the ratio in the intensity of the metabolites that are increase in Hep-G2 control relatively to Aramé treated cells, positive values in blue, negative in orange.

Preprints (www.preprints.org) | NOT PEER-REVIEWED | Posted: 9 May 2023 doi:10.20944/preprints202305.0631.v1

Hep-G2 metabolites MS negative mode	Control	Aramé
PS(16:0/0:0) (PS16)	4817	655
2-Hydroxydodecanoic acid (HD)	5908	807
phosphorylserine (PS)	4618	701
Alisine (A)	1619	299
5-hydroxyeicosatetraenoic acid (5-H)	153368	39211
2-Dodecylbenzenesulfonic acid (2-D)	148603	42759
Coenzyme A (CoA)	16957	4931
2E-Hexenedioylcarnitine (2E-H)	7323	2545
C75 trans(C75)	18763	8075
1-(9Z-Octadecenoyl)-sn-glycero-3-Phosphoethanolamine (P18)	40511	21807
Hypoxanthine (HPX)	3358	14436
Uridine (U)	5189	18536
16-Feruloyloxypalmitic acid (16-FP)	1760	4930
2-[4-[(E)-1-(4-hydroxyphenyl)-2-phenyl-but-1-enylphenyl] acetic acid (AA)	1490	4042
8-Amino-2-(3,4-dihydroxyphenyl)-3-hydroxy-6-methyl-chromone (Chromone)	1733	3947
4-Nitrophenol (4-NF)	1882	4163
1-(3-Ethylsulfinylcyclohexyl)-2-methyl-3-[2-[(5-methyl-2-thienyl)sulfonylamino]ethyl]guanidine (G)	8932	22258

(**A**)

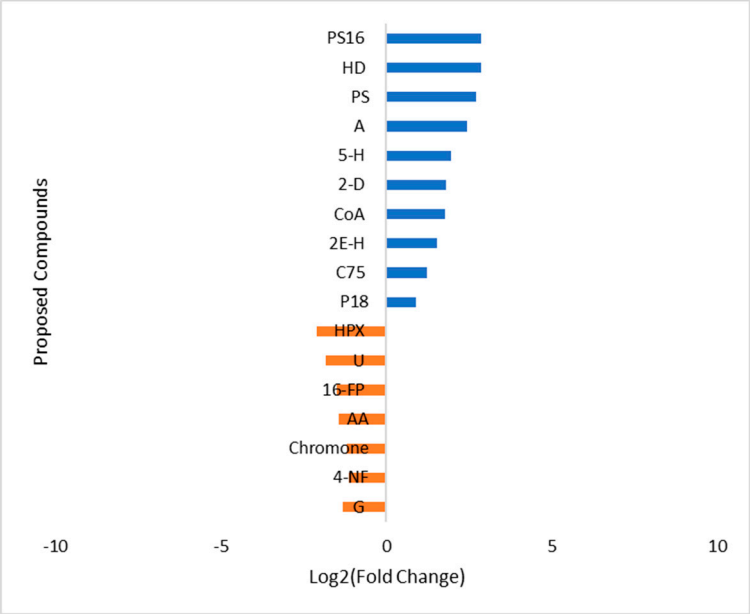

(**B**)

Figure 6. (A) Heatmap of intensity of the identified metabolites in negative mode that vary in the presence or absence of Aramé, in Hep-G2 cells, based on mean intensities ($p < 0.05$). Control is Hep-G2 cells only with culture medium and Aramé is the Hep-G2 cells in contact 24 h with 0.3 mg/mL of Aramé extract. (B) Log_2(Fold Change) represents the ratio in the intensity of the metabolites that are increase in Hep-G2 control relatively to Aramé treated cells, positive values in blue, negative in orange.

It was noted, also by PLS plots analysis (Figures S1 and S2c)), that in both type of cells the more important metabolites altered due to cells exposure to Aramé were mostly vitamins, phospholipids or related fatty acids metabolites and, also amino acids or peptides. Other type of metabolites was seen to be decreased in exposed cells, such as reduced glutathione (GSH), one of the most important scavengers of reactive oxygen species (ROS) [51] On the contrary, nucleotides as uridine (U) and hypoxanthine (HPX), an important metabolite from the purine metabolism often associated also to metabolic disorders [52] were seen to increase in the extract treated cells.

Preprints (www.preprints.org) | NOT PEER-REVIEWED | Posted: 9 May 2023 doi:10.20944/preprints202305.0631.v1

A pathway enrichment analysis of the obtained data was performed using MetaboAnalyst 5.0 tool and, in Figure 7 it is presented the metabolic pathways estimated to be affected by exposure to the Aramé extract in Caco-2 and Hep-G2 cells.

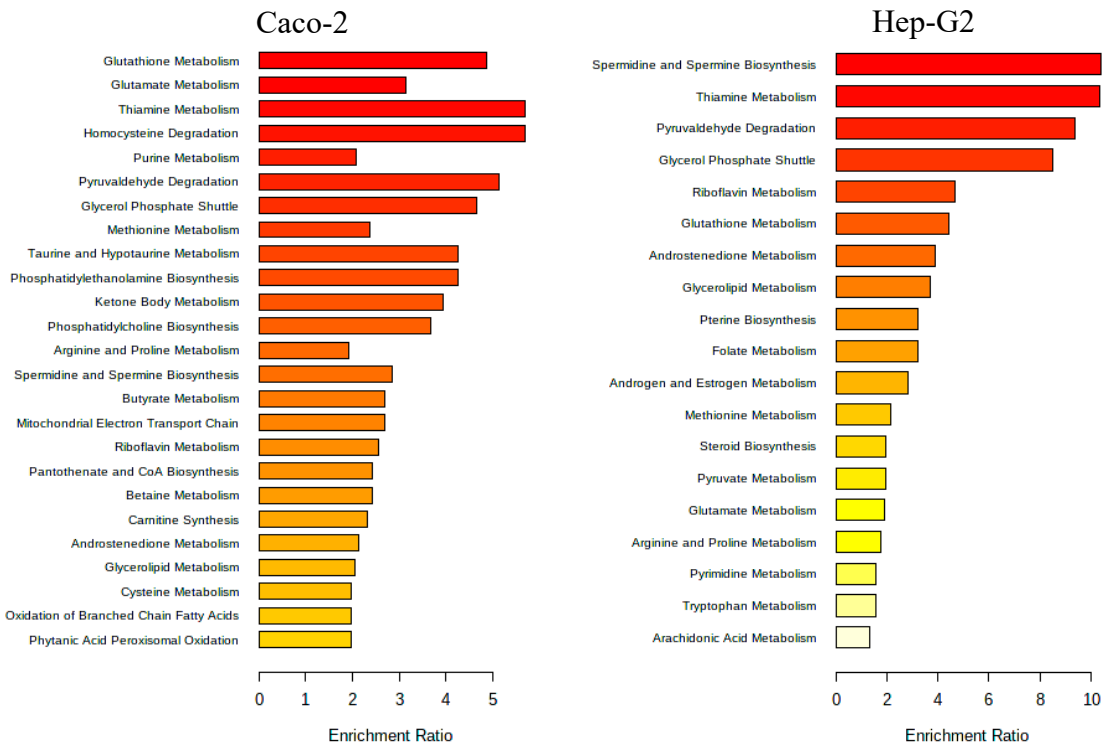

Figure 7. Metabolic pathways positively affected by the Aramé extract presence for Caco-2 and Hep-G2 cells. Obtained by MetaboAnalyst 5.0 Pathway Enrichment – analysis of significantly different metabolites between groups ($p < 0.05$). The enrichment rate is calculated as the number of hits between a particular metabolic pathway divided by the expected number of hits.

As can be seen from Figure 7, the metabolic pathways most affected in both types of cells when exposed to Aramé extract, are those associated to lipid metabolism, such as phospholipids, and fatty acid metabolism. Also, pathways of amino acid metabolism, cofactors and vitamins and energy metabolism of cellular respiration, namely catabolism or oxidation were identified to be altered when cells are exposed to the Aramé extract.

Modifications in several of these pathways have been associated to CVDs besides hypercholesterolemia and, oxidative stress. Sulfur amino acid pathways were reported as associated to the risk of CVDs [8,53]. Sulfur amino acid pathways such as, homocysteine degradation pathway, methionine and cysteine metabolism are related pathways. Within the body tissues, the metabolism of methionine and cysteine determines the concentrations of several metabolites, including coenzyme A, glutathione, and taurine [54–57]. In the cells treated with Aramé extract a decrease in the level of GSH was detected relatively to the control cells, which can be associated to a higher utilization rate of this metabolite inside the treated cells, a mechanism important to prevent oxidative stress. A modification in glutathione metabolism was seen in Hep-G2 cells exposed to a brown seaweed *Fucus vesiculosus* extract [58].

The metabolism of sulfur amino acids has also an impact on the synthesis of fatty acids and phospholipids [53]. These metabolites are important for cell membrane, especially for shielding the cells from oxidative stress, preventing several disorders such as CVDs, metabolic conditions, and neurodegenerative disorders [59]. It was seen that there were differences in the level and type of phospholipids and fatty acids between control and Aramé exposed cells. Phosphatidylcholine (PC) and phosphatidylethanolamine (PE) are major phospholipids in mammalian membrane and its modifications are reported to modify the cell membrane behavior [60] which may restrict cell

Preprints (www.preprints.org) | NOT PEER-REVIEWED | Posted: 9 May 2023 doi:10.20944/preprints202305.0631.v1

membrane fluidity, thus interfering with permeation processes and/or protecting from damages. Also, PC is the major phospholipid component of lipoproteins, and PE its precursor, reduction of PC/PE level is reported to significantly lower the levels of circulating very low-density lipoproteins (VLDLs) [61], this reduction was observed in Aramé treated cells.

The spermidine and spermine biosynthesis is also often associated to the ability to protect against CVDs [62], as these polyamines can act as anti-inflammatory, antioxidants, and free radical scavengers [63] and are also associated to the glutathione metabolism. In Aramé exposed cells a higher level of spermine was detected when compared with the control cells.

Purine metabolism was also seen to be elevated in Arame Hep-G2 and Caco-2 treated cells with accumulation of hypoxanthine (HPX), inosine (I) and deoxyinosine (D), these are products of ATP catabolism. Modifications in the purine pools in the cells is often exploited as a therapeutic target against several diseases such as cancer [64] and gout [65] and also central nervous system disorders [66].

In Hep-G2 cells exposed to Aramé extract, the thiamine metabolism was seen to be affected with a lower level of thiamine (vitamin B1) in treated cells relatively to the control cells. It may be suggested that in extract treated Hep-G2 cells, thiamine pool can be depleted due to high metabolic rate, which increased the need of this vitamin, due to the thiamine diphosphate coenzyme role in the energy metabolism of carbohydrates, lipids and amino acids [67]. It is known that under certain stress conditions, the intracellular thiamine pool is depleted, while increasing oxidative stress tolerance [68].

- Nori extract

The same type of evaluation was performed for the metabolites, after 24 h exposure to Nori extract of Caco-2 cells when compared with metabolites from non-exposed Caco-2 cells (Control). The statistical analysis is showed in Supplementary Information S3, both for the MS negative and positive mode. In the heatmaps, Figures 8A and 9A the statistically different metabolites tentatively identified using the previous mentioned databases are shown and colored from green to red for visualizing the differences in its abundance between control and extract treated cells. In the log_2(Fold change) plots, Figures 8B and 9B, representing the ratio between control cells metabolites abundance and Nori exposed cells, the more abundant metabolites in control cells are represented by the positive blue bars and the metabolites more abundant in Nori exposed cells in orange bars.

Caco-2 metabolites MS positive mode	Control	Nori
Phenacylamine (PCN)	37263	339
(1,4-dimethyl-4-propylheptyl)-(2-methylbutyl)amine (DPHMA)	464590	138209
Dibenzyl-[4-(3,7-ditert-butyl-4H-diazepin-5-yl)phenyl]amine (DINA)	65	40627
Acetylcholine (Ach)	2461	41993
6-(ethylthio)-1-(2-hydroxyethoxymethyl)-5-methyl-pyrimidine-2,4-quinone (Quinone)	914	11619
Aplidiasphingosine (APG)	2269	7509
(1S,2R)-1-[3-(methylthio)-1H-pyrazol-5-yl]propane-1,2,3-triol (Triol)	1362	4270
Cys-Pro	1408	2983
3-[7-[4-(2-acetamido-4-methyl-thiazol-5-yl)sulfonylpiperazino]-5-methyl-[1,2,4]triazolo[1,5-a]pyrimidin-6-yl]ethyl ester propionic acid (Prop)	2997	5660
ε-Caprolactam (ε-C)	269131	466393
Oleamide (OEA)	64986	100476
Palmitic Amide (PA)	29569	47171

(**A**)

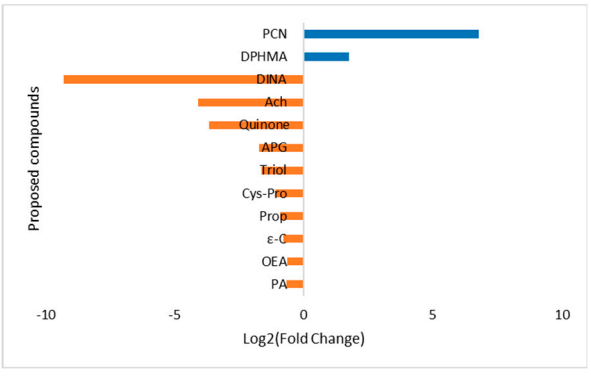

(**B**)

Figure 8. (A) Heatmap of proposed compounds that vary in the presence or absence of Nori, in Caco-2 cells in positive mode, based on mean intensities ($p < 0.05$). Control is Caco-2 cells only with culture medium and Nori is Caco-2 cells in contact 24 h with a solution of 0.3 mg/mL of Nori extract. (B) Log_2(Fold Change) represents the ratio in the intensity of the metabolites that are increase in extract treated cells relatively to the control cells identified metabolites, positive values in blue, negative in orange.

Preprints (www.preprints.org) | NOT PEER-REVIEWED | Posted: 9 May 2023 doi:10.20944/preprints202305.0631.v1

Caco-2 metabolites MS negative mode	Control	Nori
1-[1-(2-Dodekoxyethoxy)ethoxy]ethyl hydrogen sulfate (DEHS)	48491	21639
2-[3-[3-[3-(3-Octoxypropoxy)propoxy]propoxy]propoxy]ethyl hydrogen sulfate (OPEHS)	17235	7703
2-Dodecylbenzenesulfonic acid (2-D)	147569	78783
2-keto-N-[6-(4-neopentylpiperazino)-3-pyridyl]-2-(2-phenyl-5,6,7,8-tetrahydroindolizin-3-yl)acetamide (CMIDA)	391	84212
2-hydroxy-10-undecanoic acid (HUA)	175	4316
2-Hydroxydodecanoic acid (HD)	795	7516
Undecanedioic Acid (UA)	5051	27136
(1S)-N-(4-Ethylcyclohexyl)-2-[(methylthio)oxyperoxymethyl]cyclopropanecarboxamide (CPCD)	1379	4551
2-[2-[2-(Dihexylamino)-2-keto-ethoxy]ethoxy]-N,N-dihexyl-acetamide (DMIDA)	1237	2864

(**A**)

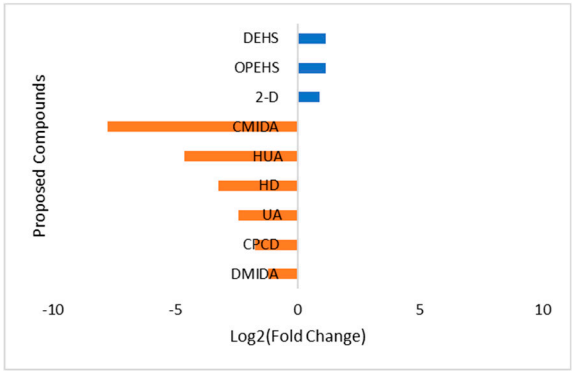

(**B**)

Figure 9. (A) Heatmap of proposed compounds that vary in the presence or absence of Nori, in Caco-2 cells in negative mode, based on mean intensities ($p < 0.05$). Control is Caco-2 cells only with culture medium and Nori is Caco-2 cells in contact 24 h with a solution of 0.3 mg/mL of Nori extract. (B) Log_2(Fold Change) represents the ratio in the intensity of the metabolites that are increase in extract treated cells relatively to the control cells identified metabolites, positive values in blue, negative in orange.

The same type of data analysis and evaluation was made for comparing the metabolites in Hep-G2 cells exposed to Nori extract with the metabolites from non-exposed Hep-G2 control cells. The statistical analysis is showed in Supplementary Information S4, both for the MS negative and positive mode. The heatmaps obtained after tentative identification of significantly variant metabolites are shown in Figures 10A and 11A for MS positive and negative mode and the log_2(Fold change) plots, Figures 10B and 11B.

Hep-G2 metabolites MS positive mode	Control	Nori
Benzylpenicilloyl-Cysteine (BPO-cys)	49783	13595
1-Palmitoylphosphatidylcholin (PPC)	40748	13457
Thiamine (B1)	9766	3276
1-(9Z-Octadecenoyl)-sn-glycero-3-Phosphoethanolamine (PE 18)	41442	13941
Phosphatidylethanolamine (PE 16)	30109	11067
Glutathione (GSH)	94977	37910
Glutathione, oxidized (GSSG)	40801	103646
Palmitic Amide (PA)	30011	72723
Hypoxanthina (HPX)	38822	91185

(**A**)

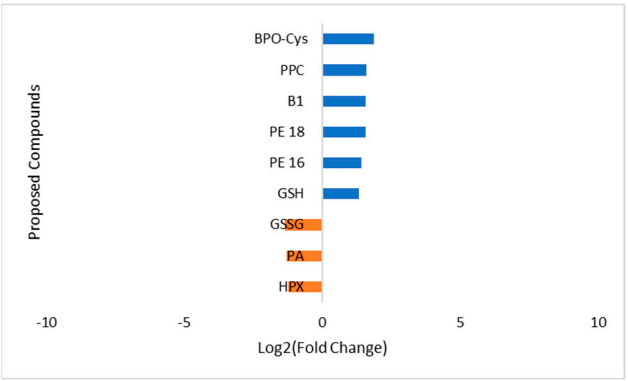

(**B**)

Figure 10. (A) Heatmap of proposed compounds that vary in the presence or absence of Nori, in Hep-G2 cells in positive mode, based on mean intensities ($p < 0.05$). Control is Hep-G2 cells only with culture medium and Nori is Hep-G2 cells in contact 24 h with a solution of 0.3 mg/mL of Nori extract. (B) Log_2(Fold Change) represents the ratio in the intensity of the metabolites that are increase in extract treated cells relatively to the control cells identified metabolites, positive values in blue, negative in orange.

Preprints (www.preprints.org) | NOT PEER-REVIEWED | Posted: 9 May 2023 doi:10.20944/preprints202305.0631.v1

Hep-G2 metabolites MS negative mode	Control	Nori
Coenzyme A (CoA)	16957	658
phosphatidylserine(16:0/0:0) (PS 16)	4817	237
2-Dodecylbenzenesulfonic acid (2-D)	148603	9411
phosphatidylserine(18:1(9Z)/0:0) (PS 18)	4618	299
1-(2-Methoxy-octadecanyl)-sn-glycer-3-phosphoserin (MPS)	29183	3217
5-hydroxyeicosatetraenoic acid (5-H)	153368	17993
2-Hydroxydodecanoic acid (HD)	5908	841
Alisine (A)	1619	231
Succinic Acid (SA)	67234	19500
Metoxyacetic Acid (McA)	220337	45156

(A)

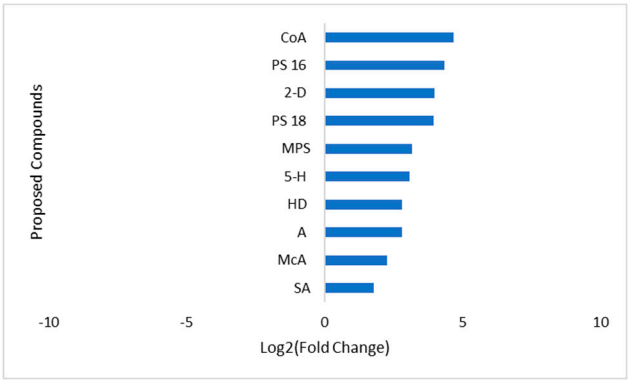

(B)

Figure 11. (A) Heatmap of proposed compounds that vary in the presence or absence of Nori, in Hep-G2 cells in negative mode, based on mean intensities ($p < 0.05$). Control is Hep-G2 cells only with culture medium and Nori is Hep-G2 cells in contact 24 h with a solution of 0.3 mg/mL of Nori extract. (B) Log_2(Fold Change) represents the ratio in the intensity of the metabolites that are increase in extract treated cells relatively to the control cells identified metabolites, positive values in blue.

By the PLS plots ((Figures S3 and S4c)) and Figures 8–11 analysis, it can be seen that overall, for both type of cells, the more important metabolites to change between control cells and Nori exposed cells, were mostly phospholipids or related fatty acids, nucleotides or related purines and pyrimidines and, vitamins and cofactors. In the case of Hep-G2 cells exposed to Nori extract it was additionally seen that, reduced glutathione (GSH) decreased, where hypoxanthine (HPX) increased, and thiamine (B1) levels decreased similarly to the previously seen for Aramé treated Hep-G2 and also for Caco-2 cells. However, in the case of cells treated with Nori the variation was less intense, as lower values of log_2(FoldChange) were obtained relatively to cells treated with Aramé.

As pathway analysis can give a more intuitive interpretation of the modifications, the metabolites were mapped to the metabolic pathways using Metaboanalyst 5.0 pathway enrichment analysis and Figure 12 was obtained.

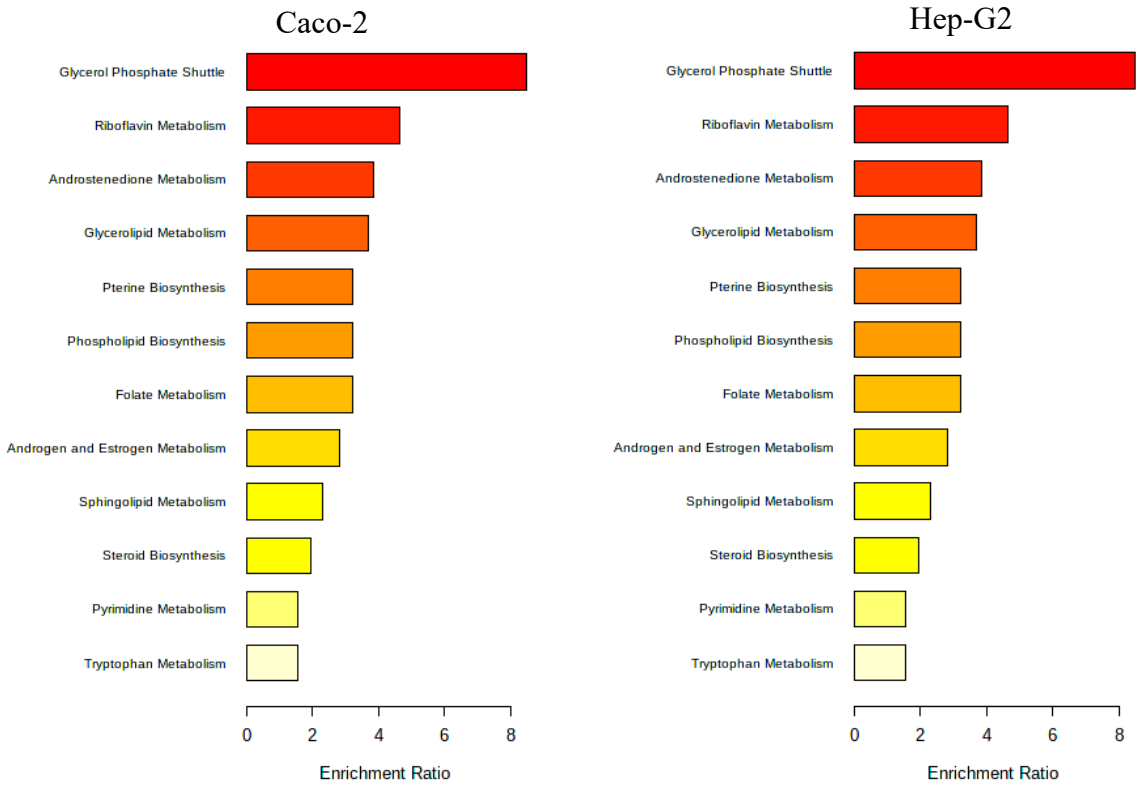

 doi:10.20944/preprints202305.0631.v1

Figure 12. Metabolic pathways positively affected by the proposed compounds, in the presence or absence of Nori, for Caco-2 and Hep-G2 cells. Obtained by MetaboAnalyst 5.0 Pathway Enrichment – analysis of significantly different metabolites between groups ($p < 0.05$). The enrichment rate is calculated as the number of hits between a particular metabolic pathway divided by the expected number of hits.

In Figure 12, the pathway enrichment analysis identified that the most affected metabolic pathways in both cell types due to contact with Nori extract were, lipid metabolism pathways, amino acids, cofactors and vitamins and energy metabolism pathways, as seen also for cells of exposed to the Aramé extract.

As it was mentioned for Aramé treated cells, variations in cells membranes lipids seen also in Nori treated cells, are reported to be associated to modifications in cells membranes fluidity and permeation behavior [60,61] and, the possible effect on decreasing lipoproteins levels, which may have beneficial effects on plasma circulating cholesterol [62]. But in the case of cells treated with Nori the variation was less intense, as lower values of $\log_2$(FoldChange) were obtained relatively to cells treated with Aramé.

In Nori treated cells it was additionally seen an increase relatively to the non-exposed cells in amide derived metabolites, such as 2-keto-N-[6-(4-neopentylpiperazino)-3-pyridyl]-2-(2-phenyl-5,6,7,8-tetrahydroindolizin-3-yl) (CMIDA). Also occurred variation in the level of amines metabolites, such as (1,4-dimethyl-4-propylheptyl)-(2-methylbutyl) amine (DPHMA) decreasing in Nori treated cells, as opposed to fatty acid amides, oleamide (OEA) and palmitic amide (PA) increasing relatively to the control. Both these types of metabolites may be related to modifications in the metabolism of lipids, proteins, and amino acids due to exposure to the Nori extract. In the case of fatty acid amides, it was already reported that Hep-G2 metabolites were modified by a *Fucus vesiculosus* extract [58].

Also, in the case of the amino acid tryptophan metabolism, Caco-2 cells treated with Nori extract were seen to increase the levels of quinone derived metabolites often associated to this pathway, again this was also seen but at a higher extent for Hep-G2 and Caco-2 cells treated with Aramé. The formation of these type of metabolites, after cells exposure to the extract, may be associated to cell protection, as the quinone moiety is highly reactive, thus prescribed against several diseases [69].

4. Discussion

The potential of marine origin products for prevention or treatment of diseases is still largely unexplored, including seaweeds. As some seaweeds and derived products are already available as nutraceuticals or claimed as functional foods, it is urgent to demonstrate and further clarify their effects on consumers health.

The results here reported have demonstrated that the often-consumed brown seaweed Aramé and red seaweed Nori extracts have effective potential against hypercholesterolemia one of the main factors associated to the risk of CVDs. Both the extracts have demonstrated the capacity to reduce the cholesterol *de novo* synthesis in the liver by inhibiting HMGR enzyme, a target for hypercholesterolemia treatment. Aramé extract showed a better performance than Nori extract for the same concentration, suggested to be associated to its higher levels of phenolic compounds and eckol type phlorotannin's. Additionally, both the extracts showed the capacity to reduce cholesterol permeation in the gastrointestinal barrier, also a target of hypercholesterolemia drug ezetimibe. Nevertheless, it was demonstrated for the first time that Nori extract interferes with ezetimibe effect in the intestinal lining. It was also demonstrated that the compounds of Aramé and Nori extract could permeate the gastrointestinal barrier *in vitro*, having the potential to move towards other body cells, tissues, or organs, hypothetically reaching the liver to inhibit HMGR.

To complement these results, an untargeted metabolomic analysis was carried out in intestinal Caco-2 and liver Hep-G2 cell lines to elucidate the mechanism of action associated to both seaweeds consumption. Our findings clearly demonstrated variations occurring in Aramé and Nori extracts exposed cells and enlightened that these could be associated to health benefits, particularly towards metabolic and other disorders, such as CVDs and oxidative related diseases.

 doi:10.20944/preprints202305.0631.v1

The cell's metabolome in contact with the extracts showed an increase or decrease in several metabolites and these were related to alterations in cell's major pathways, such as lipids, amino acids, vitamins, and nucleotides pathways. Using either of the extracts the analyzed cell lines showed a decrease in GSH relatively to the control cells, possibly due to a higher utilization rate of this metabolite inside of treated cells, suggesting the enhancement of cells' antioxidant mechanisms. Modifications in lipids could be overall associated to changes in cells membranes, but particularly a decrease in PC and PE levels, suggesting this could contribute to reduce the formation of circulating VLDL by these cells. Other type of alterations in key metabolites, such as spermine, quinone derivatives and vitamin B1, with antioxidant and anti-inflammatory potential, could be associated to protection against CVDs and other diseases and improvement of cells oxidative stress tolerance. Though some modifications were seen in cells exposed to either of the extracts, these were more robust at Aramé treated cells than in Nori exposed cells.

5. Conclusions

In conclusion, we have presented scientific evidence about the effect of brown seaweed Aramé and red seaweed Nori extracts for managing hypercholesterolemia. Both extracts demonstrated to be efficient for the reduction of cholesterol, either targeting cholesterol *de novo* biosynthesis and additionally the permeation in intestinal lining, showing a similar effect as the drugs often prescribed. In order to fully explore the potential of these seaweeds extracts for hypercholesterolemia treatment, further research is necessary to understand pharmacokinetic and pharmacodynamic properties or to establish the adequate dosage for therapeutic products. It is noteworthy however that the incorporation of Aramé and Nori seaweeds in a healthy and balanced diet stands as an effective way to prevent hypercholesterolemia and to promote health. These applications, were likewise, herein scientifically demonstrated by our metabolomic findings *in vitro*, which showed that these seaweeds extract impact in the cell's pathways possibly will be advantageous for cells protection against several disorders, including CVDs.

Supplementary Materials: Figure S1 - Analysis of compounds that vary in the presence or absence of Aramé, for Caco-2 cells, in positive (1) and negative (2) mode. a) volcano plot; b) PCA plot; c) PLS plot. DPHMA - (1,4-dimethyl-4-propylheptyl) -(2-methylbutyl)amine; HPX -Hypoxanthine; Prop - 3-[7-[4-(2-acetamido-4-methyl-thiazol-5-yl)sulfonylpiperazino]-5-methyl-[1,2,4]triazolo[1,5-a]pyrimidin-6-yl]ethyl ester propionic acid; I – Inosine; CO – Choline; AMP - Adenosine Monophosphate; L-N - L-Norleucine; MPN - 1-Monopalmitin; GSH – Glutathione; SAD - Succinyl Adenosine; BPO-Cys - Benzylpenicilloyl-Cysteine; DHES - 1-[1-(2-Dodekoxyethoxy)ethoxy]ethyl hydrogen sulfate; Acetamida - 2-keto-N-[6-(4-neopentylpiperazino)-3-pyridyl]-2-(2-phenyl-5,6,7,8-tetrahydroindolizin-3-yl)acetamide; Cet - Cetoleucine; U -Uridine; MPS - 1-(2-Metoxy-octadecanyl)-sn-glycero-3-phosphoserine, GN – Guanosine; PG 22 - PG (22:6(4Z,7Z,10Z,13Z,16Z,19Z)/0:0); 2E-H - 2E-Hexenedioylcarnitine; PE 18 - 1-(9Z-Octadecenoyl)-sn-glycero-3-Phosphoethanolamine; C75 – C75 trans. Figure S2 - Analysis of compounds that vary in the presence or absence of Aramé, for Hep-G2 cells, in positive (1) and negative (2) mode. a) volcano plot; b) PCA plot; c) PLS plot. ε-C – ε- Caprolactam; HPX -Hypoxanthine; Prop - 3-[7-[4-(2-acetamido-4-methyl-thiazol-5-yl)sulfonylpiperazino]-5-methyl-[1,2,4]triazolo [1,5-a]pyrimidin-6-yl]ethyl ester propionic acid; DPHMA - (1,4-dimethyl-4-propylheptyl) -(2-methylbutyl)amine; GSH – Glutathione; I – Inosine; 5′ – Deoxy – 5′ - 5′-methylthioadenosine ; 5-H - 5-hydroxyeicosatetraenoic acid; 2-D - 2-Dodecylbenzenesulfonic acid; PE 18 - 1-(9Z-Octadecenoyl)-sn-glycero-3-Phosphoethanolamine; U – Uridine; G - 1-(3-Ethylsulfinylcyclohexyl)-2-methyl-3-[2-[(5-methyl-2-thienyl)sulfonylamino]ethyl]guanidine ; C75 – C75 trans; CoA – coenzyme A. Figure S3 - Analysis of compounds that vary in the presence or absence of Nori, for Caco-2 cells, in positive (1) and negative (2) mode. a) volcano plot; b) PCA plot; c) PLS plot; d) log2(fold change) chart. DPHMA - (1,4-dimethyl-4-propylheptyl) -(2-methylbutyl) amine; ε-C – ε- Caprolactam; Ach - Acetylcholine; PCN - Phenacylamine; OEA - Oleamide; DINA - Dibenzyl-[4-(3,7-ditert-butyl-4H-diazepin-5-yl)phenyl]amine; CMIDA - 2-keto-N-[6-(4-neopentylpiperazino)-3-pyridyl]-2-(2-phenyl-5,6,7,8-tetrahydroindolizin-3-yl)acetamide; 2-D - 2-Dodecylbenzenesulfonic acid; DEHS - 1-[1-(2-Dodekoxyethoxy)ethoxy]ethyl hydrogen sulfate; UA - Undecanedioic Acid; OPEHS - 2-[3-[3-[3-(3-Octoxypropoxy)propoxy]propoxy]propoxy]ethyl hydrogen sulfate; HUA - 2-hydroxy-10-undecanoic acid. Figure S4 - Analysis of compounds that vary in the presence or absence of Nori, for Hep-G2 cells, in positive (1) and negative (2) mode. a) volcano plot; b) PCA plot; c) PLS plot. AD - Adenosine; L-N - L-Norleucine; GSSH – Glutathione; DPHMA - (1,4-dimethyl-4-propylheptyl) -(2-methylbutyl) amine; GSH – Glutathione; PA – Palmitic Amide; HPX – Hypoxanthine; BPO-Cys - Benzylpenicilloyl-Cysteine; PE18 - 1-(9Z-Octadecenoyl)-sn-glycero-3-Phosphoethanolamine; PPC - 1-Palmitoylphosphatidylcholin; 2-D - 2-Dodecylbenzenesulfonic acid; 5-H - 5-

hydroxyeicosatetraenoic acid; McA - Methoxyacetic Acid; SA - 2-[[2-acetamido-3-carboxy-propanoyl]amino] succinic acid.

Author Contributions: Conceptualization and methodology R.P.; software, R.P.; validation, R.P.; formal analysis and investigation, M.C.; resources, R.P.; data curation, M.C.; writing—M.C.; writing—review and editing, R.P.; visualization, R.P.; supervision, R.P.; project administration, R.P.; funding acquisition, R.P. All authors have read and agreed to the published version of the manuscript.

Funding: This research was funded by Centro de Química Estrutural is a Research Unit (RU) funded by Fundação para a Ciência e Tecnologia, projects UIDB/00100/2020 and UIDP/00100/2020. Authors also acknowledge financial support by project PTDC/BIA-BQM/28355/2017.

Acknowledgments: The authors would like to acknowledge the scientific support of Professor Maria Luísa Serralheiro at the Biosystems & Integrative Sciences Institute (BioISI) MassSpec Facility, Faculdade de Ciências, Universidade de Lisboa, UIDB/04046/2020 and UIDP/04046/2020.

Conflicts of Interest: The authors declare no conflict of interest.

References

1. Amante, C.; Esposito, T.; Luccheo, G.; Luccheo, L.; Russo, P.; Del Gaudio, P. *Life* **2022**, *12*, doi:10.3390/life12081162.
2. Organization, W.H. Cardiovascular Diseases. Available online: https://www.who.int/cardiovascular_diseases/about_cvd/en/. (accessed on 12 march 2023)
3. Martinez-Hervas, S.; Ascaso, J.F. Hypercholesterolemia. In *Encyclopedia of Endocrine Diseases (Second Edition)*, Huhtaniemi, I., Martini, L., Eds.; Academic Press: Oxford, 2019; pp. 320-326.
4. Civeira, F.; Arca, M.; Cenarro, A.; Hegele, R.A. A mechanism-based operational definition and classification of hypercholesterolemia. *Journal of Clinical Lipidology* **2022**, *16*, 813-821, doi:https://doi.org/10.1016/j.jacl.2022.09.006.
5. André, R.; Pacheco, R.; Bourbon, M.; Serralheiro, M.L. Brown Algae Potential as a Functional Food against Hypercholesterolemia: Review. *Foods* **2021**, *10*, doi:10.3390/foods10020234.
6. Nordestgaard, B.G.; Nicholls, S.J.; Langsted, A.; Ray, K.K.; Tybjærg-Hansen, A. Advances in lipid-lowering therapy through gene-silencing technologies. *Nat Rev Cardiol* **2018**, *15*, 261-272, doi:10.1038/nrcardio.2018.3.
7. Qian, J.; Li, Z.; Zhang, X.; Chen, J.; Ding, C.; Yang, P.; Liu, Y.; Shi, M.; Ren, X.; Ge, J. Efficacy and Tolerability of Ezetimibe/Atorvastatin Fixed-dose Combination Versus Atorvastatin Monotherapy in Hypercholesterolemia: A Phase III, Randomized, Active-controlled Study in Chinese Patients. *Clinical Therapeutics* **2022**, *44*, 1282-1296, doi:10.1016/j.clinthera.2022.08.013.
8. Database, H.M. Cholesterol. Available online: (accessed on
9. Luo, J.; Yang, H.; Song, B.L. Mechanisms and regulation of cholesterol homeostasis. *Nat Rev Mol Cell Biol* **2020**, *21*, 225-245, doi:10.1038/s41580-019-0190-7.
10. Ressaissi, A.; Attia, N.; Pacheco, R.; Falé, P.L.; Serralheiro, M.L.M. Cholesterol transporter proteins in HepG2 cells can be modulated by phenolic compounds present in Opuntia ficus-indica aqueous solutions. *Journal of Functional Foods* **2020**, *64*, 103674, doi:https://doi.org/10.1016/j.jff.2019.103674.
11. Burmaoglu, S.; Yilmaz, A.O.; Taslimi, P.; Algul, O.; Kilic, D.; Gulcin, I. Synthesis and biological evaluation of phloroglucinol derivatives possessing α-glycosidase, acetylcholinesterase, butyrylcholinesterase, carbonic anhydrase inhibitory activity. *Archiv der Pharmazie* **2018**, *351*, 1700314, doi:https://doi.org/10.1002/ardp.201700314.
12. Phan, B.A.; Dayspring, T.D.; Toth, P.P. Ezetimibe therapy: mechanism of action and clinical update. *Vasc Health Risk Manag* **2012**, *8*, 415-427, doi:10.2147/vhrm.s33664.
13. Battaggia, A.; Donzelli, A.; Font, M.; Molteni, D.; Galvano, A. Clinical efficacy and safety of Ezetimibe on major cardiovascular endpoints: systematic review and meta-analysis of randomized controlled trials. *PLoS One* **2015**, *10*, e0124587, doi:10.1371/journal.pone.0124587.
14. Cardiology, A.C.o. Ezetimibe: The lower the LDL-C, the better (even for total cardiovascular events). Available online: Ezetimibe: The Lower the LDL-C, the Better (Even for Total Cardiovascular Events) - American College of Cardiology (acc.org) (accessed on 1st March).
15. Ward, N.C.; Watts, G.F.; Eckel, R.H. Statin Toxicity. *Circulation Research* **2019**, *124*, 328-350, doi:10.1161/CIRCRESAHA.118.312782.
16. Mach, F.; Ray, K.K.; Wiklund, O.; Corsini, A.; Catapano, A.L.; Bruckert, E.; De Backer, G.; Hegele, R.A.; Hovingh, G.K.; Jacobson, T.A.; et al. Adverse effects of statin therapy: perception vs. the evidence - focus on glucose homeostasis, cognitive, renal and hepatic function, haemorrhagic stroke and cataract. *Eur Heart J* **2018**, *39*, 2526-2539, doi:10.1093/eurheartj/ehy182.
17. Collins, R.; Reith, C.; Emberson, J.; Armitage, J.; Baigent, C.; Blackwell, L.; Blumenthal, R.; Danesh, J.; Smith, G.D.; DeMets, D.; et al. Interpretation of the evidence for the efficacy and safety of statin therapy. *Lancet* **2016**, *388*, 2532-2561, doi:10.1016/s0140-6736(16)31357-5.

18. Duan, Y.; Gong, K.; Xu, S.; Zhang, F.; Meng, X.; Han, J. Regulation of cholesterol homeostasis in health and diseases: from mechanisms to targeted therapeutics. *Signal Transduction and Targeted Therapy* **2022**, *7*, 265, doi:10.1038/s41392-022-01125-5.
19. Pinto, S.; Gaspar, M.M.; Ascensão, L.; Faísca, P.; Reis, C.P.; Pacheco, R. Nanoformulation of Seaweed Eisenia bicyclis in Albumin Nanoparticles Targeting Cardiovascular Diseases: In Vitro and In Vivo Evaluation. *Marine Drugs* **2022**, *20*, doi:10.3390/md20100608.
20. El-Tantawy, W.H.; Temraz, A. Natural products for controlling hyperlipidemia: review. *Arch Physiol Biochem* **2019**, *125*, 128-135, doi:10.1080/13813455.2018.1441315.
21. Hunter, P.M.; Hegele, R.A. Functional foods and dietary supplements for the management of dyslipidaemia. *Nat Rev Endocrinol* **2017**, *13*, 278-288, doi:10.1038/nrendo.2016.210.
22. Mohd Sairazi, N.S.; Sirajudeen, K.N.S. Natural Products and Their Bioactive Compounds: Neuroprotective Potentials against Neurodegenerative Diseases. *Evid Based Complement Alternat Med* **2020**, *2020*, 6565396, doi:10.1155/2020/6565396.
23. Santini, A.; Novellino, E. Nutraceuticals in hypercholesterolaemia: an overview. *Br J Pharmacol* **2017**, *174*, 1450-1463, doi:10.1111/bph.13636.
24. Rigogliuso, S.; Campora, S.; Notarbartolo, M.; Ghersi, G. Recovery of Bioactive Compounds from Marine Organisms: Focus on the Future Perspectives for Pharmacological, Biomedical and Regenerative Medicine Applications of Marine Collagen. *Molecules* **2023**, *28*, doi:10.3390/molecules28031152.
25. Coelho, M.; Duarte, A.P.; Pinto, S.; Botelho, H.M.; Reis, C.P.; Serralheiro, M.L.; Pacheco, R. Edible Seaweeds Extracts: Characterization and Functional Properties for Health Conditions. *Antioxidants* **2023**, *12*, doi:10.3390/antiox12030684.
26. Gómez-Guzmán, M.; Rodríguez-Nogales, A.; Algieri, F.; Gálvez, J. Potential Role of Seaweed Polyphenols in Cardiovascular-Associated Disorders. *Mar Drugs* **2018**, *16*, doi:10.3390/md16080250.
27. Yamagata, K. Prevention of cardiovascular disease through modulation of endothelial cell function by dietary seaweed intake. *Phytomedicine Plus* **2021**, *1*, 100026, doi:https://doi.org/10.1016/j.phyplu.2021.100026.
28. Meinita, M.D.; Harwanto, D.; Choi, J.-S. Seaweed Exhibits Therapeutic Properties against Chronic Diseases: An Overview. *Applied Sciences* **2022**, *12*, doi:10.3390/app12052638.
29. Collins, K.G.; Fitzgerald, G.F.; Stanton, C.; Ross, R.P. Looking Beyond the Terrestrial: The Potential of Seaweed Derived Bioactives to Treat Non-Communicable Diseases. *Mar Drugs* **2016**, *14*, doi:10.3390/md14030060.
30. Leandro, A.; Pacheco, D.; Cotas, J.; Marques, J.C.; Pereira, L.; Gonçalves, A.M.M. Seaweed's Bioactive Candidate Compounds to Food Industry and Global Food Security. *Life (Basel)* **2020**, *10*, doi:10.3390/life10080140.
31. Choudhary, B.; Chauhan, O.P.; Mishra, A. Edible Seaweeds: A Potential Novel Source of Bioactive Metabolites and Nutraceuticals With Human Health Benefits. *Frontiers in Marine Science* **2021**, *8*.
32. Mahadevan, K. Seaweeds: A sustainable food source. 2015; pp. 347-364.
33. Peñalver, R.; Lorenzo, J.M.; Ros, G.; Amarowicz, R.; Pateiro, M.; Nieto, G. Seaweeds as a Functional Ingredient for a Healthy Diet. *Mar Drugs* **2020**, *18*, doi:10.3390/md18060301.
34. Jung, H.A.; Roy, A.; Jung, J.H.; Choi, J.S. Evaluation of the inhibitory effects of eckol and dieckol isolated from edible brown alga Eisenia bicyclis on human monoamine oxidases A and B. *Arch Pharm Res* **2017**, *40*, 480-491, doi:10.1007/s12272-017-0904-3.
35. Kim, H.J.; Dasagrandhi, C.; Kim, S.H.; Kim, B.G.; Eom, S.H.; Kim, Y.M. In Vitro Antibacterial Activity of Phlorotannins from Edible Brown Algae, Eisenia bicyclis Against Streptomycin-Resistant Listeria monocytogenes. *Indian J Microbiol* **2018**, *58*, 105-108, doi:10.1007/s12088-017-0693-x.
36. Kim, K.A.; Kim, S.M.; Kang, S.W.; Jeon, S.I.; Um, B.H.; Jung, S.H. Edible seaweed, Eisenia bicyclis, protects retinal ganglion cells death caused by oxidative stress. *Mar Biotechnol (NY)* **2012**, *14*, 383-395, doi:10.1007/s10126-012-9459-y.
37. Venkatraman, K.L.; Mehta, A. Health Benefits and Pharmacological Effects of Porphyra Species. *Plant Foods Hum Nutr* **2019**, *74*, 10-17, doi:10.1007/s11130-018-0707-9.
38. Ichihara, T.; Wanibuchi, H.; Taniyama, T.; Okai, Y.; Yano, Y.; Otani, S.; Imaoka, S.; Funae, Y.; Fukushima, S. Inhibition of liver glutathione S-transferase placental form-positive foci development in the rat hepatocarcinogenesis by Porphyra tenera (Asakusa-nori). *Cancer Lett* **1999**, *141*, 211-218, doi:10.1016/s0304-3835(99)00106-8.
39. Arantes, A.A. Inhibition of HMG-CoA redutase activity and cholesterol permeation through Caco-2 cells by caffeoylquinic acids from *Vernonia condensata* leaves. **2016**, *26*, 738-743.
40. Theodoridis, G.A.; Gika, H.G.; Want, E.J.; Wilson, I.D. Liquid chromatography-mass spectrometry based global metabolite profiling: a review. *Anal Chim Acta* **2012**, *711*, 7-16, doi:10.1016/j.aca.2011.09.042.
41. Worley, B.; Powers, R. Multivariate Analysis in Metabolomics. *Curr Metabolomics* **2013**, *1*, 92-107, doi:10.2174/2213235x11301010092.

42. Climent, E.; Benaiges, D.; Pedro-Botet, J. Hydrophilic or Lipophilic Statins? *Front Cardiovasc Med* **2021**, *8*, 687585, doi:10.3389/fcvm.2021.687585.
43. Zhao, J.; Cao, Q.; Xing, M.; Xiao, H.; Cheng, Z.; Song, S.; Ji, A. Advances in the Study of Marine Products with Lipid-Lowering Properties. *Mar Drugs* **2020**, *18*, doi:10.3390/md18080390.
44. Yoon, N.Y.; Kim, H.R.; Chung, H.Y.; Choi, J.S. Anti-hyperlipidemic effect of an edible brown algae, Ecklonia stolonifera, and its constituents on poloxamer 407-induced hyperlipidemic and cholesterol-fed rats. *Arch Pharm Res* **2008**, *31*, 1564-1571, doi:10.1007/s12272-001-2152-8.
45. Feng, D.; Ohlsson, L.; Duan, R.D. Curcumin inhibits cholesterol uptake in Caco-2 cells by down-regulation of NPC1L1 expression. *Lipids Health Dis* **2010**, *9*, 40, doi:10.1186/1476-511x-9-40.
46. Larregieu, C.A.; Benet, L.Z. Drug discovery and regulatory considerations for improving in silico and in vitro predictions that use Caco-2 as a surrogate for human intestinal permeability measurements. *Aaps j* **2013**, *15*, 483-497, doi:10.1208/s12248-013-9456-8.
47. Ramos, A.A.; Almeida, T.; Lima, B.; Rocha, E. Cytotoxic activity of the seaweed compound fucosterol, alone and in combination with 5-fluorouracil, in colon cells using 2D and 3D culturing. *J Toxicol Environ Health A* **2019**, *82*, 537-549, doi:10.1080/15287394.2019.1634378.
48. Eid, S.Y.; Althubiti, M.A.; Abdallah, M.E.; Wink, M.; El-Readi, M.Z. The carotenoid fucoxanthin can sensitize multidrug resistant cancer cells to doxorubicin via induction of apoptosis, inhibition of multidrug resistance proteins and metabolic enzymes. *Phytomedicine* **2020**, *77*, 153280, doi:https://doi.org/10.1016/j.phymed.2020.153280.
49. Murata, N.; Keitoku, S.; Miyake, H.; Tanaka, R.; Shibata, T. Evaluation on Intestinal Permeability of Phlorotannins Using Caco-2 Cell Monolayers. *Natural Product Communications* **2022**, *17*, 1934578X211070415, doi:10.1177/1934578X211070415.
50. Corona, G.; Ji, Y.; Anegboonlap, P.; Hotchkiss, S.; Gill, C.; Yaqoob, P.; Spencer, J.P.; Rowland, I. Gastrointestinal modifications and bioavailability of brown seaweed phlorotannins and effects on inflammatory markers. *Br J Nutr* **2016**, *115*, 1240-1253, doi:10.1017/s0007114516000210.
51. Reed, M.C.; Thomas, R.L.; Pavisic, J.; James, S.J.; Ulrich, C.M.; Nijhout, H.F. A mathematical model of glutathione metabolism. *Theoretical Biology and Medical Modelling* **2008**, *5*, 8, doi:10.1186/1742-4682-5-8.
52. Hira, H.S.; Samal, P.; Kaur, A.; Kapoor, S. Plasma level of hypoxanthine/xanthine as markers of oxidative stress with different stages of obstructive sleep apnea syndrome. *Ann Saudi Med* **2014**, *34*, 308-313, doi:10.5144/0256-4947.2014.308.
53. Blachier, F.; Andriamihaja, M.; Blais, A. Sulfur-Containing Amino Acids and Lipid Metabolism. *J Nutr* **2020**, *150*, 2524s-2531s, doi:10.1093/jn/nxaa243.
54. KEGG. Glutathione. Available online: https://www.genome.jp/pathway/map00480 (accessed on 16th July).
55. KEGG. Alanine, aspartate and
56. glutamate metabolism Available online: glutamate metabolism - Reference pathway (genome.jp) (accessed on 16th July).
57. KEGG. Taurine and hypotaurine
58. metabolism Available online: metabolism - Reference pathway (genome.jp) (accessed on 16th July).
59. Stipanuk, M.H.; Ueki, I. Dealing with methionine/homocysteine sulfur: cysteine metabolism to taurine and inorganic sulfur. *J Inherit Metab Dis* **2011**, *34*, 17-32, doi:10.1007/s10545-009-9006-9.
60. André, R.; Guedes, R.; López, J.; Serralheiro, M.L. Untargeted metabolomic study of HepG2 cells under the effect of Fucus vesiculosus aqueous extract. *Rapid Commun Mass Spectrom* **2021**, *35*, e9197, doi:10.1002/rcm.9197.
61. Rehman, T.; Shabbir, M.A.; Inam-Ur-Raheem, M.; Manzoor, M.F.; Ahmad, N.; Liu, Z.W.; Ahmad, M.H.; Siddeeg, A.; Abid, M.; Aadil, R.M. Cysteine and homocysteine as biomarker of various diseases. *Food Sci Nutr* **2020**, *8*, 4696-4707, doi:10.1002/fsn3.1818.
62. Li, Z.; Agellon, L.B.; Allen, T.M.; Umeda, M.; Jewell, L.; Mason, A.; Vance, D.E. The ratio of phosphatidylcholine to phosphatidylethanolamine influences membrane integrity and steatohepatitis. *Cell Metab* **2006**, *3*, 321-331, doi:10.1016/j.cmet.2006.03.007.
63. Deschamps, C.L.; Connors, K.E.; Klein, M.S.; Johnsen, V.L.; Shearer, J.; Vogel, H.J.; Devaney, J.M.; Gordish-Dressman, H.; Many, G.M.; Barfield, W.; et al. The ACTN3 R577X Polymorphism Is Associated with Cardiometabolic Fitness in Healthy Young Adults. *PLoS One* **2015**, *10*, e0130644, doi:10.1371/journal.pone.0130644.
64. Qiu, Y.; Li, L.; Guo, X.; Liu, J.; Xu, L.; Li, Y. Exogenous spermine inhibits high glucose/oxidized LDL-induced oxidative stress and macrophage pyroptosis by activating the Nrf2 pathway. *Exp Ther Med* **2022**, *23*, 310, doi:10.3892/etm.2022.11239.
65. Yu, Z.; Jiao, Y.; Zhang, J.; Xu, Q.; Xu, J.; Li, R.; Yuan, W.; Guo, H.; Sun, Z.; Zheng, L. Effect of Serum Spermidine on the Prognosis in Patients with Acute Myocardial Infarction: A Cohort Study. *Nutrients* **2022**, *14*, doi:10.3390/nu14071394.
66. Liu, J.; Hong, S.; Yang, J.; Zhang, X.; Wang, Y.; Wang, H.; Peng, J.; Hong, L. Targeting purine metabolism in ovarian cancer. *Journal of Ovarian Research* **2022**, *15*, 93, doi:10.1186/s13048-022-01022-z.

67. Said, H.M.; Reidling, J.C.; Ortiz, A. Cellular and molecular aspects of thiamin uptake by human liver cells: studies with cultured HepG2 cells. *Biochimica et Biophysica Acta (BBA) - Biomembranes* **2002**, *1567*, 106-112, doi:https://doi.org/10.1016/S0005-2736(02)00606-5.
68. Nascimento, F.P.; Macedo-Júnior, S.J.; Lapa-Costa, F.R.; Cezar-dos-Santos, F.; Santos, A.R.S. Inosine as a Tool to Understand and Treat Central Nervous System Disorders: A Neglected Actor? *Frontiers in Neuroscience* **2021**, *15*.
69. Eshak, E.S.; Arafa, A.E. Thiamine deficiency and cardiovascular disorders. *Nutr Metab Cardiovasc Dis* **2018**, *28*, 965-972, doi:10.1016/j.numecd.2018.06.013.
70. Tunc-Ozdemir, M.; Miller, G.; Song, L.; Kim, J.; Sodek, A.; Koussevitzky, S.; Misra, A.N.; Mittler, R.; Shintani, D. Thiamin confers enhanced tolerance to oxidative stress in Arabidopsis. *Plant Physiol* **2009**, *151*, 421-432, doi:10.1104/pp.109.140046.
71. Bolton, J.L.; Dunlap, T. Formation and Biological Targets of Quinones: Cytotoxic versus Cytoprotective Effects. *Chem Res Toxicol* **2017**, *30*, 13-37, doi:10.1021/acs.chemrestox.6b00256.